Molecular Biology Reports (2024) 51:988
https://doi.org/10.1007/s11033-024-09927-2

ORIGINAL ARTICLE

Innate immunity gene *Nod2* protects mice from orthotopic breast cancer

Serdar Gurses[1,2] · Nivya Varghese[1] · Dipika Gupta[1]

Received: 22 July 2024 / Accepted: 9 September 2024

Abstract

Background *Nod2* is involved in innate immune responses to bacteria, regulation of metabolism, and sensitivity to cancer. A *Nod2* polymorphism is associated with breast cancer, but the role of *Nod2* in the development and progression of breast cancer is unknown.

Methods Here, we tested the hypothesis that *Nod2* protects mice from breast cancer using the 4T1 orthotopic model of mammary tumorigenesis. WT and $Nod2^{-/-}$ mice were injected with 4T1 mammary carcinoma cells and the development of tumors was monitored. A detailed analysis of the tumor transcriptome was performed and genes that were differentially expressed and pathways that were predicted to be altered between WT and $Nod2^{-/-}$ mice were identified. The activation of key signaling molecules involved in metabolism and development of cancer was studied.

Results Our data demonstrate that $Nod2^{-/-}$ mice had a higher incidence and larger tumors than WT mice. $Nod2^{-/-}$ mice had increased expression of genes that promote DNA replication and cell division, and decreased expression of genes required for lipolysis, lipogenesis, and steroid biosynthesis compared with WT mice. $Nod2^{-/-}$ mice also had lower expression of genes required for adipogenesis and reduced levels of lipids compared with WT mice. The tumors in $Nod2^{-/-}$ mice had decreased expression of genes associated with PPARα/γ signaling, increased activation of STAT3, decreased activation of STAT5, and no change in the activation of ERK compared with WT mice.

Conclusions We conclude that *Nod2* protects mice from the 4T1 orthotopic breast tumor, and that tumors in $Nod2^{-/-}$ mice are predicted to have increased DNA replication and cell proliferation and decreased lipid metabolism compared with WT mice.

Keywords *Nod2* · Innate immunity · Breast cancer · Transcriptome · Orthotopic tumor model

Introduction

Breast cancer accounts for 25% of new cancer cases in women and is the most frequent cause of cancer-related deaths in women worldwide [1, 2]. Breast tumors exhibit large diversity in phenotype, development, and responsiveness to treatments, which results in a poor prognosis for patients [3, 4]. Genetic studies have identified a few hundred susceptibility loci associated with familial relative risk for breast cancer. However, the breast cancer heritability remains mostly unexplained, with the expectation that additional susceptibility loci will be identified [5]. This genetic complexity greatly contributes to the diversity in the pathophysiology of breast cancer and its responsiveness to chemotherapies. In addition, there are few tissue markers that can consistently diagnose breast cancer at an early stage, an important factor for improving prognosis [6]. Thus, a comprehensive gene expression profile will help develop more effective diagnostics markers and treatments for patients with breast cancer.

Nod2 is a cytoplasmic innate immunity protein, which is stimulated by bacterial peptidoglycan fragments resulting in the activation of NF-κB and MAP kinase-signaling cascades and the production of inflammatory molecules and anti-microbial peptides [7–10]. There is increasing evidence that besides bacterial peptidoglycan, Nod2 is likely activated by other ligands, including cellular ligands released during stress [11, 12]. In vivo, *Nod2* has a critical role in maintaining intestinal homeostasis and is a major susceptibility gene

✉ Dipika Gupta
dgupta@iu.edu

[1] Indiana University School of Medicine–Northwest, Gary, IN 46408, USA

[2] Present Address: The University of Texas MD Anderson Cancer Center, Houston, TX 77030, USA

Published online: 17 September 2024

for Crohn's disease [13, 14]. Furthermore, polymorphisms in *Nod2* are associated with an increased risk for colorectal cancer [15–17]. In experimental models, *Nod2* deficiency promotes the development of colitis and colorectal cancer [18], which may depend on the inhibition of Toll-like receptor (TLR)-mediated activation of NF-κB and MAPK signaling [19], though the underlying mechanism is not fully understood.

We and others have previously shown that *Nod2* protects mice from the development of diet-dependent obesity [20, 21]. *Nod2*$^{-/-}$ mice on a high-fat diet (HFD) become obese, develop steatosis, and exhibit increased expression of genes for many inflammatory molecules, compared with wild-type mice on HFD. Notably, the *Nod2*$^{-/-}$ HFD microbiota contributes to the development of obesity and steatosis in these mice [20–22]. We also recently showed that the *Nod2* deficiency results in the increased sensitivity to obesity-dependent hepatic tumorigenesis [23]. The development of liver tumors in *Nod2*$^{-/-}$ mice depends on HFD and involves increased expression of genes involved in cell proliferation, immune responses, and cholesterol biosynthesis. These *Nod2*$^{-/-}$ mice display increased infiltration of neutrophils, inflammatory monocytes, and T cells in the liver, and increased activation of STAT3 and ERK signaling molecules [23]. *Nod2* has also been shown to protect mice from the development of hepatocellular carcinoma (HCC) induced by N-nitrosodiethylamine/carbon tetrachloride or tumor xenograft [24]. In vitro, molecular changes associated with chemically induced HCC in the absence of *Nod2* depended on the increased activation of adenosine 5′-monophosphate activated protein kinase (AMPK) and apoptosis [24].

Nod2 may also be associated with increased risk for breast cancer, because the *Nod2* variant 3020insC is associated with early-onset breast cancer and increased expression of *Nod2* inhibits cell proliferation of the Hs578T breast cancer cell line [25–27]. However, the role of *Nod2* in the development of breast cancer and the underlying mechanisms are poorly understood.

In the current study, we tested the hypothesis that *Nod2* protects mice from breast cancer. Using an orthotopic model, we demonstrate that *Nod2*$^{-/-}$ mice are more susceptible to the development of 4T1 breast tumors. We analyzed the tumor transcriptome and identified pathways that are predicted to be differentially regulated between WT and *Nod2*$^{-/-}$ mice. 4T1 tumors in *Nod2*$^{-/-}$ mice had significantly increased expression of genes involved in DNA replication and repair and cell proliferation and significantly decreased expression of genes involved in lipolysis, lipogenesis, steroid biosynthesis, and adipogenesis compared with WT mice. The tumors in *Nod2*$^{-/-}$ mice displayed increased expression of genes in ErbB signaling but decreased expression of genes in PPARα/γ and stress response signaling. *Nod2*$^{-/-}$ mice also showed increased activation of STAT3, reduced activation of STAT5 and no change in the activation of ERK compared with WT mice. Based on these changes, we suggest that *Nod2* protects mice from transplanted tumors and that the orthotopic tumor model in *Nod2*$^{-/-}$ mice provides a viable in vivo system to study the development of breast cancer and the effectiveness of therapeutics.

Materials and methods

Mice and induction of breast tumors

We used WT and *Nod2*$^{-/-}$ mice on a BALB/c background for all experiments. The original founder WT BALB/c mice were obtained from Harlan–Sprague–Dawley. *Nod2*$^{-/-}$ mice on BALB/c background were described previously [20, 23]. All mice were bred and kept under conventional pathogen-free conditions in the same room in our facility to minimize any environmental differences. Mice were kept on Teklad #7001 chow diet. For each experiment, mice from several different cages and breeder pairs were used. The BALB/c background of knockout mice and their negative status for all common viral and bacterial pathogens and parasites were confirmed as previously described [47]. All experimental protocols with mice were approved by the Indiana University School of Medicine-Northwest Institutional Animal Care and Use Committee. All methods were carried out in accordance with relevant guidelines and regulations. All methods are reported in accordance with Animal Research: Reporting of In Vivo Experiments (ARRIVE) guidelines (https://arriveguidelines.org).

We used 4T1 cells (ATCC CRL-2539) to establish orthotopic tumors in mice. 4T1 is a mammary carcinoma cell line, which rapidly establishes tumors when injected into the mammary tissue of mice, and thus, provides a well-established orthotopic breast cancer model [28, 29]. There is one other cell line, TS/A, which develops syngeneic mammary tumors in BALB/c mice [30]. However, compared with 4T1, the TS/A cell line has not been used as extensively in research and there are fewer resources. We, thus, used 4T1 cell for our current experiments. 4T1 cells were cultured according to ATCC guidelines. For transplant, cells around 60–80% confluency were detached, centrifuged, and resuspended in HBSS at 2×10^5 cells/ml. Each mouse was injected with 1×10^4 cells into the mammary fat pad under the abdominal mammary gland and tumor growth was monitored every day. Tumors became visible on day 5 following the injection and mice were sacrificed on day 9. At the time of sacrifice, tumors were measured using Mitutoyo Vernier caliper for height, width, and length. In cases when the height of the tumor could not be measured, the smallest measurement was taken as the height. The formula $V = (\pi \times W \times H \times L)/6$ was used to calculate the volume of

each tumor. Blood and tumor samples were collected for biochemical and molecular assays.

RNA extraction, sequencing, RT-qPCR, and data processing

To identify genes that were differentially expressed between the tumors in WT and *Nod2*$^{-/-}$ mice, we analyzed the total RNA population by RNA sequencing. RNA was isolated from the excised tumors of individual mice using the TRIZOL method (InVitrogen), followed by purification on RNeasy spin columns using the Qiagen RNeasy Mini Kit [20, 23]. RNA sequencing and initial analysis were performed at the Center for Genomics and Bioinformatics, Indiana University Bloomington. Reads were adapter trimmed and quality filtered using Trimmomatic ver. 0.33 (http://www.usadellab.org/cms/?page=trimmomatic), with the cutoff threshold for average base quality score set at 20 over a window of 3 bases. Reads shorter than 20 bases post-trimming were excluded. More than 98% of the reads (on average 24.1 million read pairs per library) passed the quality filters. Cleaned reads were mapped to the mouse reference genome GRCm38 (gencode M16), using TopHat2 ver. 2.1.1 (https://doi.org/https://doi.org/10.1186/gb-2013-14-4-r36). Approximately 95.2% of the total cleaned reads mapped to the reference and more than 96.5% of those mapped uniquely. All supporting transcriptomic data have been deposited with NCBI's Gene Expression Omnibus.

Differential expression with statistical analysis was calculated using the software DESeq2 [20, 23, 31]. The fold change was computed for *Nod2*$^{-/-}$ relative to WT, and genes that had a fold change of ≥ 2 (increased or decreased) and FDR $P \leq 0.05$ were considered as biologically and significantly different between the 2 groups. We analyzed the data using Ingenuity Pathway Analysis software (Qiagen) to identify Gene Ontology biological functions, pathways and diseases that are predicted to be differentially activated between WT and *Nod2*$^{-/-}$ mice.

The change in gene expression was confirmed for select genes by RT-qPCR. cDNA was synthesized using the ThermoFisher High-Capacity cDNA Reverse Transcription Kit (with random primers) and then amplified with gene specific primers using the ThermoFisher Fast SYBR Green Master Mix. The genes and primers used for qPCR are shown in Supplementary Table S5. The expression was calculated using the comparative cycle threshold method with three housekeeping genes (*Actb*, *Gusb*, and *Gapdh*).

Network analysis of differentially expressed genes

Protein–protein interactions among the differentially expressed genes in adipogenesis were predicted using Search Tool for the Retrieval of Interacting Genes (STRING) software v11.0 (http://string-db.org) with the combined score set at 0.7. STRING uses genomic context information text mining, experimental data, and database searches as sources for interaction criteria [32].

Lipid assays

Tumor homogenates were prepared as described previously and the total amount of cholesterol and triglyceride was quantified using fluorometric kits from BioVision Inc [20].

Western blots

Tumor samples homogenates were prepared and analyzed by Western blots as described previously [23]. Proteins were separated on 12% SDS-PAGE gels and transferred to PVDF membrane. The membrane was incubated with the primary antibody overnight and with the secondary antibody for 1 h, washed with TBST, and then developed with the SuperSignal™ West Pico Plus Chemiluminescent or SuperSignal™ West Femto Maximum Sensitivity Substrate. The chemiluminescent signal was captured using Azure 400 and band intensities were measured using ImageJ. All antibodies were purchased from Cell Signaling Technology. All primary antibodies were rabbit monoclonals and were diluted 1:500 for phospho-Stat5 (Tyr694, Cat. # 4322) and 1:1000 for phospho-STAT3 (Tyr705, Cat. # 9145), phospho-p44/42 MAPK (Erk1/2) (Thr202/Tyr204, Cat. # 4370), and β-Actin (Cat. # 4970). Anti-rabbit IgG, HRP-linked secondary antibody (Cat. # 7074) was diluted 1:1000.

Statistical analysis

Differential expression of genes with statistical analysis was calculated using the software DESeq2 and is described in the RNA sequencing section. The significance of differences in pathway analysis was determined using the Ingenuity Pathway Analysis (Qiagen). Other quantitative results are presented as means ± SEM and the significance of differences was determined by the Student's *t*-test or by Chi square. The *N* and *P* values are indicated in the Figures and Tables; $P \leq 0.05$ was considered significant. The heatmaps were generated using Java TreeView and represent individual and mean fold changes in *Nod2*$^{-/-}$ mice relative to WT mice, after converting < 1 ratios to negative fold differences using the formula: (−1)/ratio.

Results

Nod2 protects from orthotopic 4T1 breast tumors

To test our hypothesis that *Nod2* protects mice from the development of breast tumors, we injected 4T1 cells into the abdominal mammary fat pad of WT and *Nod2*$^{-/-}$ female mice. 4T1 is a mammary carcinoma cell line derived from BALB/c mice. 4T1 cells rapidly establish tumors when injected into the mammary tissue of BALB/c mice, and thus provide a well-studied syngeneic orthotopic breast cancer model [28, 29]. Tumors were visible by day 5 after the injection and on day 9 mice were sacrificed and tumors were extracted, measured, and analyzed. *Nod2*$^{-/-}$ mice developed larger tumors; the tumor weight and volume were significantly higher in *Nod2*$^{-/-}$ mice than in WT mice (Fig. 1A–C). There was also a significant difference in the incidence of tumor development between WT and *Nod2*$^{-/-}$ mice; 100% of *Nod2*$^{-/-}$ mice developed tumors, whereas only 50% of WT mice developed tumors (Fig. 1D). These results indicate that *Nod2* protects mice from the development of the orthotopic 4T1 mammary tumors.

Development of 4T1 breast tumors in *Nod2*$^{-/-}$ mice is associated with differential expression of genes in lipid metabolism, cell cycle, and cancer pathways

To unravel the molecular mechanisms underlying the development of breast tumors in *Nod2*$^{-/-}$ mice in an unbiased manner, we performed RNAseq using total RNA from the tumors of WT and *Nod2*$^{-/-}$ mice injected with 4T1 cells. Compared with WT mice, *Nod2*$^{-/-}$ mice had significantly altered expression of over 3000 genes with at least 5% FDR (false discovery rate, $P \leq 0.05$). Of these 3000 genes, over 800 genes had ≥ twofold increase in expression and over 2000 genes had ≤ twofold decrease in expression in *Nod2*$^{-/-}$ mice (Supplementary Fig. S1). We analyzed the differentially expressed genes using Ingenuity Pathway Analysis software (Qiagen) to identify Gene Ontology (GO) biological functions and diseases that are altered between WT and *Nod2*$^{-/-}$ mice [23]. Based on the number of differentially expressed genes, the most altered biological functions between WT and *Nod2*$^{-/-}$ mice were lipid metabolism and cell cycle (Table 1). The top three diseases that were predicted to be significantly altered between WT and *Nod2*$^{-/-}$ mice were cancer, endocrine system disorders, and reproductive system diseases (Table 1).

We further analyzed our transcriptomics data for specific pathways associated with the biological functions and diseases that were significantly altered between WT and *Nod2*$^{-/-}$ mice (Table 2). Gene expression analysis predicted that tumors in *Nod2*$^{-/-}$ mice had increased DNA replication, DNA repair, and cell cycle and its regulation (Table 2). By contrast, tumors in *Nod2*$^{-/-}$ mice were predicted to have decreased biosynthesis and hydrolysis pathways for fatty acids, triglycerides, and cholesterol (Table 2). Tumors in *Nod2*$^{-/-}$ mice were also predicted to have reduced adipogenesis. We analyzed our transcriptomics data for differential activation of regulatory molecules and signaling pathways

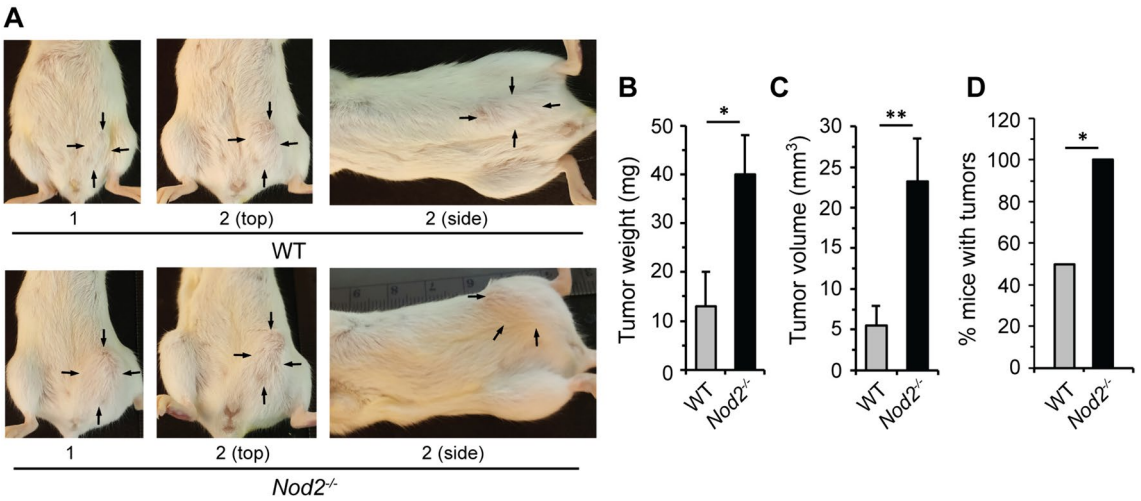

Fig. 1 *Nod2*$^{-/-}$ mice are more susceptible to the development of 4T1 orthotopic tumors than WT mice. WT and *Nod2*$^{-/-}$ female mice were injected with 4T1 cells into the mammary fat pad and tumor growth was monitored every day. Mice were sacrificed on day 9 following the transplant, and tumors were measured for weight, height, and length and the volume was calculated. **A** Representative images of two WT (1 and 2) and *Nod2*$^{-/-}$ (1 and 2) mice with tumors (indicated by black arrows), **B** average tumor weight ± SEM, **C** average tumor volume ± SEM, and **D** percent of mice with tumors. $N = 10–12$ mice/group. Significance of difference **B**, **C** by *t*-test and **D** by Chi-square. *$P \leq 0.05$ and **$P \leq 0.001$ *Nod2*$^{-/-}$ versus WT

Table 1 Top Gene Ontology biological functions and diseases significantly altered in the 4T1 tumors of *Nod2*$^{-/-}$ mice compared with WT mice

Gene ontology biological functions and diseases		Number of genes	*P*-value range
Biological function	Lipid metabolism	405	1.51E-07 to 1.23E-30
	Cell cycle	345	1.42E-07 to 6.22E-24
Disease	Cancer	1584	1.52E-07 to 1.70E-37
	Endocrine system disorders	1348	1.67E-07 to 1.80E-32
	Reproductive system diseases	1080	1.52E-07 to 9.27E-29

Table 2 Top Gene Ontology pathways that are predicted to be significantly altered in the 4T1 tumors in *Nod2*$^{-/-}$ mice compared with WT mice

Gene ontology pathways		*P*-value
DNA replication and repair	DNA replication	5.012E-11
	Deoxyribonucleotide de novo biosynthesis	6.760E-3
	Nucleotide excision repair	2.911E-02
	Mismatch repair	8.511E-04
	Double-strand DNA repair	3.467E-05
Cell cycle and regulation	Cyclins and cell cycle regulation	4.074E-4
	Checkpoint regulation	1.950E-05
Lipogenesis	Fatty acid biosynthesis	1.778E-05
	Triglyceride biosynthesis	1.862E-06
	Phosphatidylglycerol biosynthesis	7.244E-04
Lipolysis	Mitochondrial fatty acid oxidation	1.995E-16
	Peroxisomal beta-oxidation	1.738E-03
Steroid biosynthesis	Cholesterol biosynthesis	2.630E-05
	Estrogen biosynthesis	3.467E-03
TCA cycle & pyruvate metabolism	TCA cycle	1.738E-3
	Biosynthesis of acetyl CoA	1.023E-3
Adipocyte biology	Adipogenesis	1.445E-04
Signaling	PPARα and PPARγ	1.810E-36
	LXR/RXR	9.550E-4
	ErbB	5.010E-60
Stress response	Glutathione-mediated detoxification	3.162E-08
	Nrf2-mediated oxidative stress response	4.786E-03

between WT and *Nod2*$^{-/-}$ mice. The PPARα/PPARγ and LXR/RXR signaling pathways were predicted to be significantly inhibited, whereas the ErbB signaling pathway was predicted to be significantly elevated and glutathione-mediated detoxification and Nrf-2-mediated oxidative stress response to be significantly decreased in *Nod2*$^{-/-}$ mice compared with WT mice.

We next identified individual genes associated with these pathways with a focus on genes that have ≥ twofold increase or decrease in expression and 5% or lower FDR between the two groups of mice. The change in expression (fold change) of individual genes in *Nod2*$^{-/-}$ mice compared with WT mice is shown as heat maps and the genes are grouped together by their function/pathway (Figs. 2, 3, 4, 5). Many genes belong to multiple pathways, but in the heat maps, genes are only included in their identified primary pathway. Change in gene expression for select genes in cell cycle and lipid metabolism was confirmed by RT-qPCR (Fig. 6).

Development of 4T1 breast tumors in *Nod2*$^{-/-}$ mice is associated with increased expression of genes involved in DNA replication and repair, and in cell cycle

Based on our transcriptomic data, 4T1 tumors in *Nod2*$^{-/-}$ mice had a significantly higher expression of genes in DNA replication compared with WT mice (Table 2). Genes that code for proteins required for replication were overwhelmingly upregulated in the tumors of *Nod2*$^{-/-}$ mice and included enzymes and accessory proteins: DNA polymerases (*Pola1*, *Pola2*, *Pole*), primases (*Prim1*, *Prim2*), topoisomerases (*Top2a*, *Topbp1*), and DNA helicase (mini-chromosome maintenance complex, *Mcm2-7*, *Mcm10*) (Fig. 2 and Supplementary Table S1). Genes coding for proteins that mediate chromatin assembly and integrity (*Chaf1a*, *Chaf1b*, *Dnmt1*, *Hat1*, *Uhrf1*) were also upregulated. The expression of genes that code for proteins involved

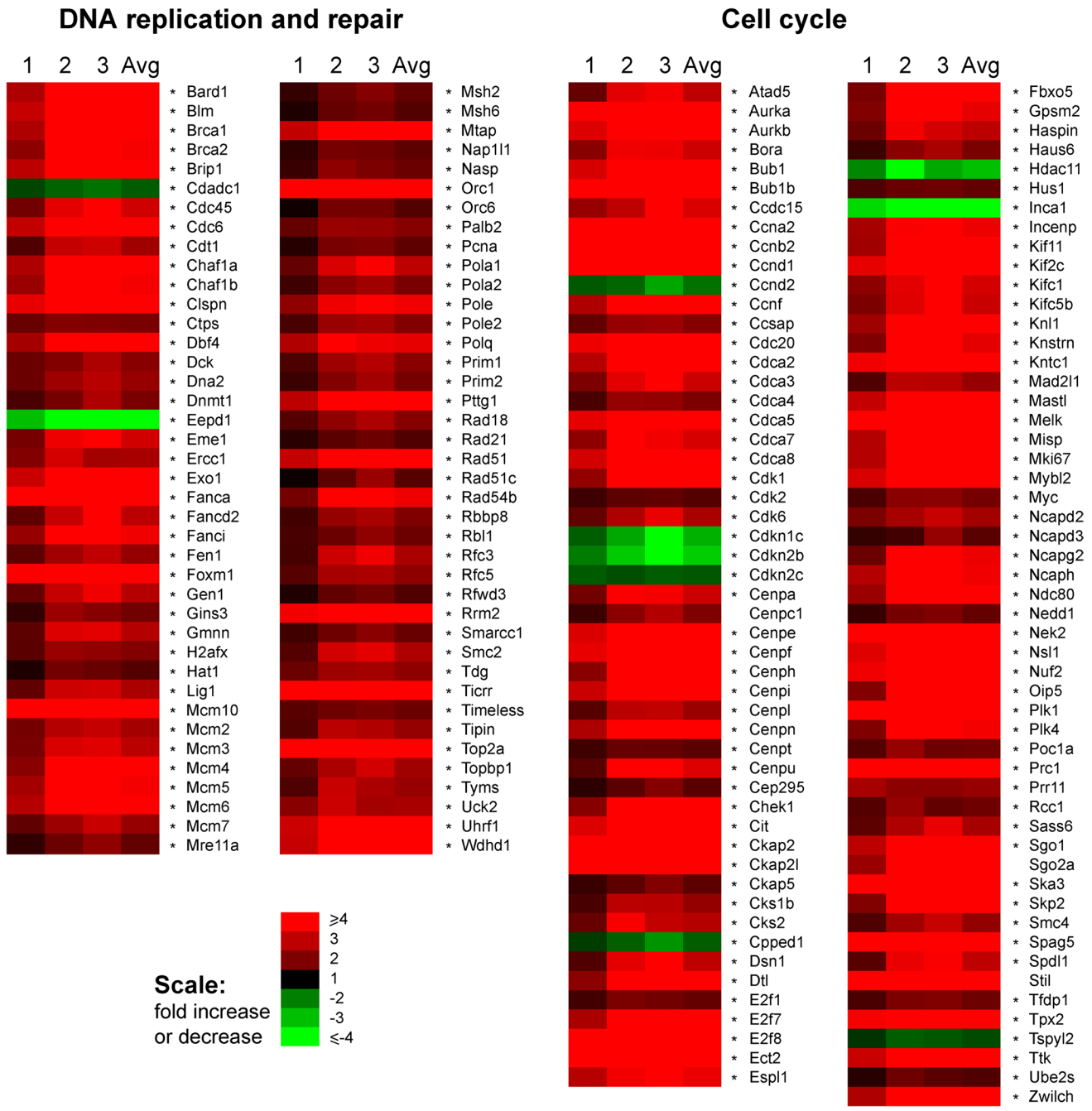

Fig. 2 The 4T1 tumors in *Nod2*$^{-/-}$ mice have increased expression of genes that promote DNA replication, repair, and cell proliferation. Heatmap representation of the fold change in gene expression in the tumors of *Nod2*$^{-/-}$ mice compared with WT mice. The genes are grouped based on pathways. The fold ratio for individual *Nod2*$^{-/-}$ mice to the average of WT mice is shown in lanes 1 to 3 and the average (Avg) fold change for all *Nod2*$^{-/-}$ mice. Asterisks indicate genes that were previously shown to be associated with cancer. Genes that have a ≥ twofold increase or decrease and with FDR $P \leq 0.05$ are included in the heatmap. $N = 3$ mice/group. The numerical data for individual and average RNA fold change (*Nod2*$^{-/-}$/WT) are shown in Supplementary Table S1

in nucleotide synthesis or salvage pathways (*Cdadc1*, *Ctps*, *Dck*, *Mtap*, *Rrm2*, *Tyms*, *Uck2*) was also significantly increased in *Nod2*$^{-/-}$ mice.

Nod2$^{-/-}$ mice had an increased expression of genes in DNA repair pathways, including nucleotide excision repair, mismatch repair, and double-stranded DNA repair pathways, compared with WT mice (Table 2). Genes in nucleotide excision repair (*Ercc1, Rad18*), mismatch repair (*Exo1*, *Msh2*, *Msh6*), double strand DNA repair (*Blm*, Brca1, Brca2, *Fancd2*, Mre11a, *Rad21*), and genes

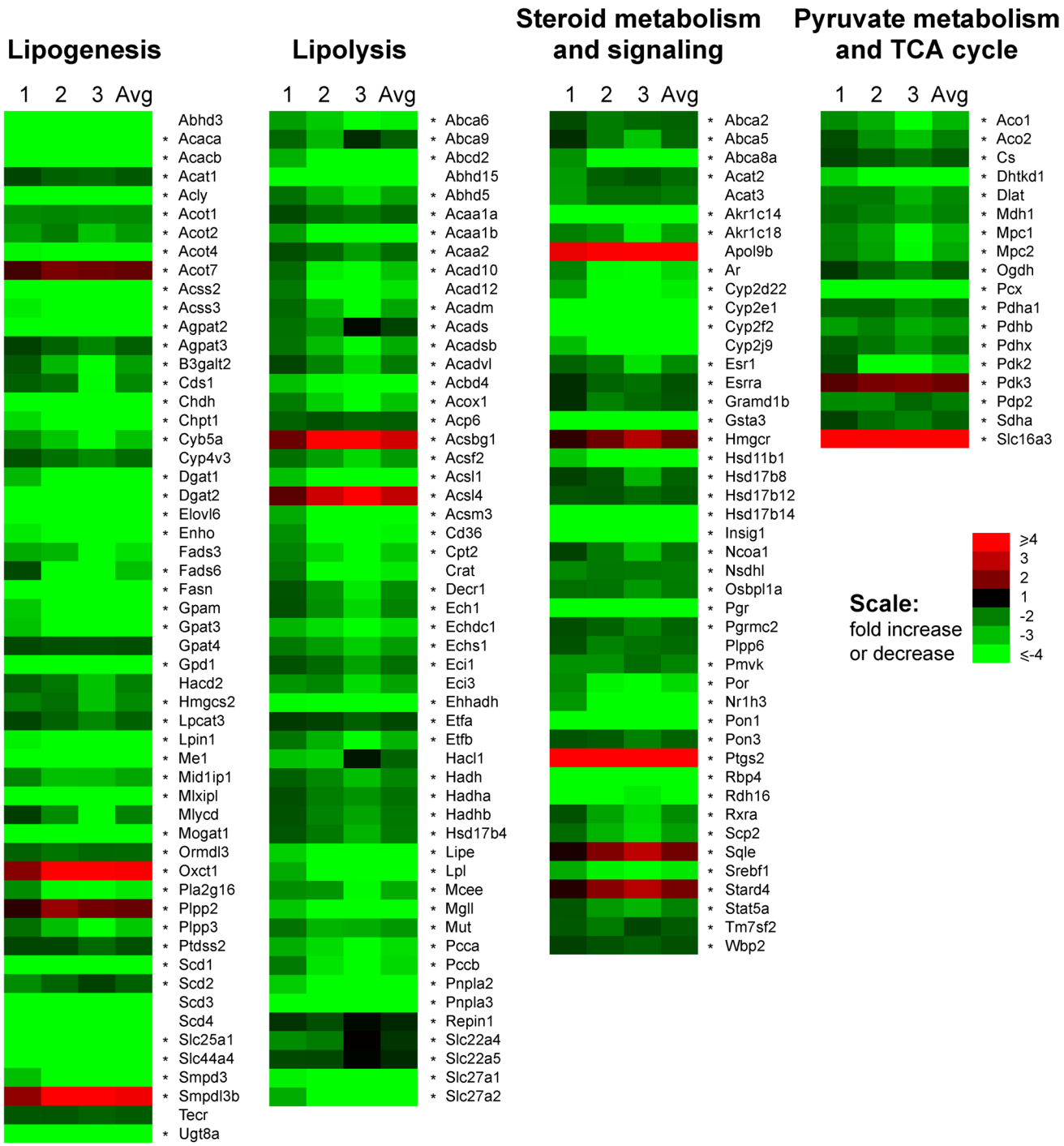

Fig. 3 The 4T1 tumors in *Nod2*$^{-/-}$ mice have decreased expression of genes for proteins in lipid metabolism, TCA cycle, and steroid biosynthesis and signaling. Heatmap representation of the fold change for gene expression in the tumors of *Nod2*$^{-/-}$ mice compared with WT mice. The genes are grouped based on pathways and calculated and presented as in Fig. 2. The numerical data for individual and average RNA fold change (*Nod2*$^{-/-}$/WT) are shown in Supplementary Table S2

that participate in more than one repair pathway (*Dna2*, *Fen1*, *Pole2*, *Rad51*, *Rad51c*, *Rad54b*, Rfc3) were upregulated in the tumors of *Nod2*$^{-/-}$ mice compared with WT mice (Fig. 2 and Supplementary Table S1).

Nod2$^{-/-}$ mice had a significantly higher expression of genes involved in the cell cycle, which includes cyclins and cell cycle regulation and checkpoint regulation compared with WT mice (Table 2). Genes that code for

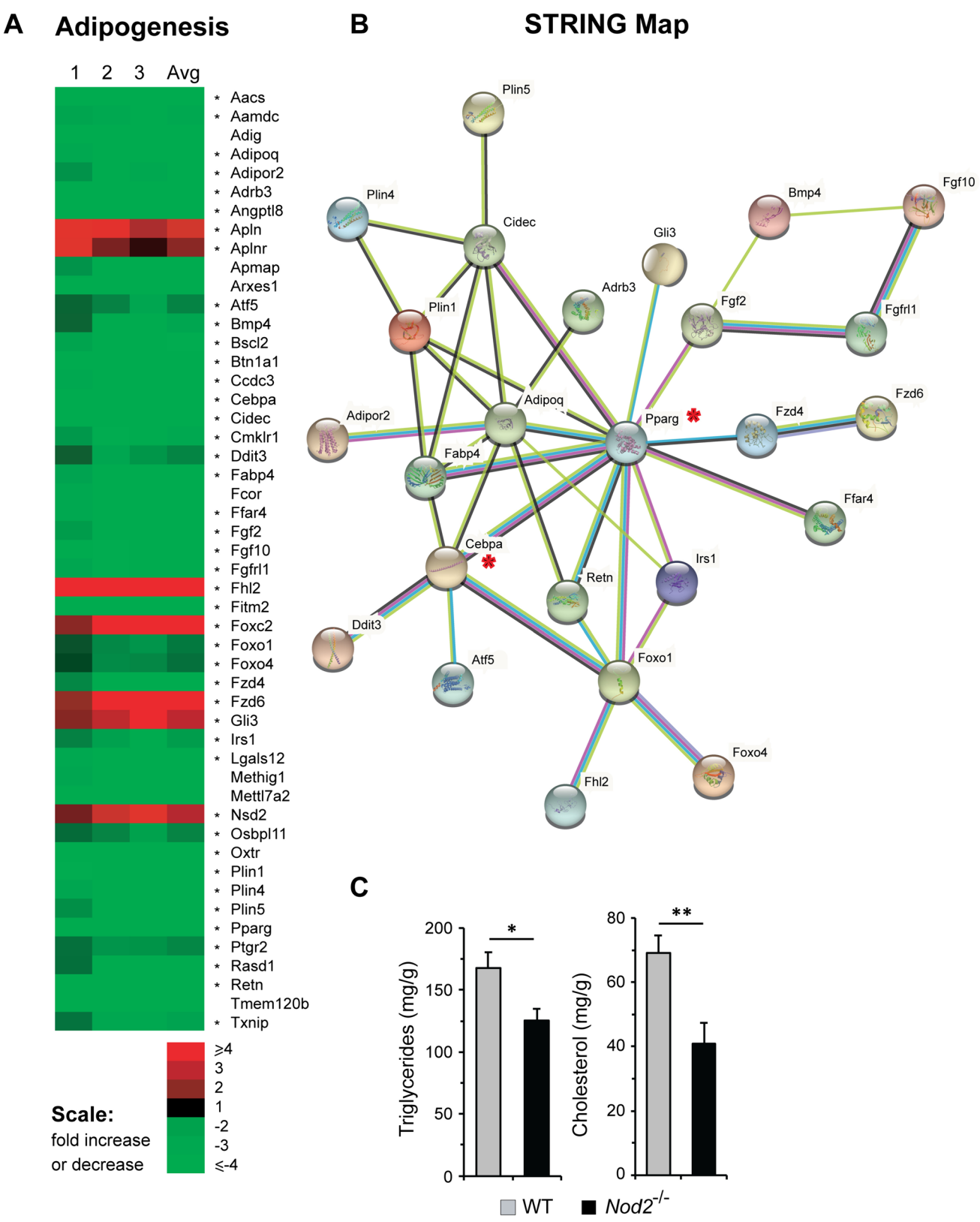

proteins required for or promoting the cell cycle were overwhelmingly upregulated in *Nod2*$^{-/-}$ mice and included genes that code for cyclins (*Ccna2*, *Ccnb2*, *Ccnd1*, *Ccnf*), cyclin-dependent kinases and accessory proteins (*Cdk1*, *Cdk2*, *Cdk6*, *Cks1b*, *Cks2*), Aurora kinases (*Aurka*, *Aurkb*), and E2F transcription factors (*Cdca4*, *E2f1*, *E2f7*, *Edf8*).

◂**Fig. 4** The 4T1 tumors in *Nod2*$^{-/-}$ mice have decreased expression of genes that promote adipogenesis, decreased PPARγ signaling, and decreased lipids. **A** Heatmap representation of the fold change for gene expression in the tumors of *Nod2*$^{-/-}$ mice compared with WT mice. The results are calculated and presented as in Fig. 2. **B** STRING analysis of genes that regulate adipogenesis and are differentially expressed between WT and *Nod2*$^{-/-}$ mice. Protein–protein interactions with a combined confidence score of 0.7 or higher are shown and interactions between only 2 proteins are excluded. The interactions between expressed proteins are indicated by the connecting lines, and darker lines represent a stronger association than lighter lines. **C** average triglyceride levels ± SEM and average cholesterol levels ± SEM in the tumors of WT and *Nod2*$^{-/-}$ mice, from two experiments. **A**, **B** $N=3$ and **C** $N=10$ mice/group. **C** Significance of difference by *t*-test, $^{*}P \leq 0.05$ *Nod2*$^{-/-}$ versus WT. The numerical data for individual and average RNA fold change (*Nod2*$^{-/-}$/WT) in **A** are shown in Supplementary Table S3

Nod2$^{-/-}$ mice had significantly higher expression of genes that code for centromere proteins, which are essential for forming the kinetochore or attachment of the chromosomes to the mitotic spindle (*Cenpa*, *Cenpc1*, *Cenpe*, *Cenpf*, *Cenph*, *Cenpi*, *Cenpl*, *Cenpn*, *Cenpt*, *Cenpu*, *Incenp*), and for several cell cycle associated ubiquitin ligases and accessory proteins required for ubiquitination (*Cdc20*, *Dtl*, *Fbxo5*, *Skp2*, *Ube2s*). *Nod2*$^{-/-}$ mice had significantly higher expression of the cell proliferation markers (*Mki67*, *Mybl2*, *Myc*) compared with WT mice (Fig. 2 and Supplementary Table S1). By contrast, there was decreased expression of several cell cycle inhibitors (*Cdkn1c*, *Cdkn2b*, *Cdkn2c*, *Cpped1*, *Hdac11*, *Inca1*, and *Tspyl2*). Increased expression of select genes in cell cycle (*Ccnb2*, *Cdk1*, *Cdk6*, *Pcna*, and *Myc*) in *Nod2*$^{-/-}$ tumors compared with WT tumors was confirmed by RT-qPCR (Fig. 6A).

These results demonstrate that the 4T1 tumors in *Nod2*$^{-/-}$ mice had increased expression of genes that promote DNA replication and cell division, which likely contributed to the higher incidence and larger 4T1 tumors in *Nod2*$^{-/-}$ mice compared with WT mice.

Development of 4T1 breast tumors in *Nod2*$^{-/-}$ mice is associated with decreased expression of genes involved in lipid and steroid metabolism and signaling

Gene expression analysis of 4T1 tumors predicted a reduction in lipid metabolism, both biosynthesis and hydrolysis, in *Nod2*$^{-/-}$ mice compared with WT mice (Table 2). *Nod2*$^{-/-}$ mice had significantly decreased expression of genes coding for enzymes in fatty acid synthesis (*Acaca*, *Acacb*, *Acly*, *Acot1*, *Acot2*, Acot4, Acot7, *Acss2*, *Fasn*) and desaturation of fatty acids (*Cyb5a*, *Cyp4b3*, *Fads3*, *Fads6*, *Scd1*, *Scd2*, *Scd3*, *Scd4*) (Fig. 3 and Supplementary Table S2). Genes coding for enzymes in phospholipid and triacylglycerol synthesis (*Agpat2*, *Agpat3*, *Chpt1*, *Dgat1*, *Dgat2*, *Gpam*, *Gpat3*, *Gpat4*, *Lpcat3*, *Lpin1*, *Mogat1*, *Ormdl3*, *Oxct1*, *Plpp2*, *Plpp3*, *Ptdss2*), and its regulators (*Me1*, *Midlip1*, *Mlxipl*) were downregulated. The expression of genes coding for enzymes in choline metabolism and its transport (*Chdh*, *Slc44a4*), the citrate transporter (Slc25a1), and genes related to ketone body metabolism (*Acat1*, *Acss3*, *Hmgcs2*, *Oxct1*) was also significantly decreased in *Nod2*$^{-/-}$ mice (Fig. 3 and Supplementary Table S2).

Nod2$^{-/-}$ mice also showed significantly decreased expression of genes involved in fatty acid oxidation and triglyceride hydrolysis. Genes coding for carnitine/acyl-carnitine transporters (*Cpt2*, *Crat*, *Slc22a4*, *Slc22a5*) and lipid transporters (*Abca6*, *Abca9*, *Abcd2*, *Cd36*) were downregulated in *Nod2*$^{-/-}$ mice compared with WT mice (Fig. 3 and Supplementary Table S2). *Nod2*$^{-/-}$ mice also had significantly decreased expression of genes coding for enzymes in mitochondrial fatty acid oxidation (*Acaa2*, *Acad10*, *Acadm*, *Acads*, *Acadsb*, *Acadvl*, *Acsl1*, *Ecsh1*, *Hadh*, *Hadha*, *Hadhb*) and peroxisomal fatty acid oxidation (*Abcd2*, *Acaa1a*, *Acaa1b*, *Acox1*, *Ech1*, *Eci3*, *Hsd17b4*). Moreover, genes coding for enzymes and their regulators in triglyceride hydrolysis (*Abhd5*, *Lipe*, *Lpl*, *Mgll*, *Pnpla2*, *Pnpla3*) and oxidation of odd-chain fatty acids (*Mcee*, *Mut*, *Pcca*, *Pccb*) were also downregulated in *Nod2*$^{-/-}$ mice (Fig. 3 and Supplementary Table S2).

Nod2$^{-/-}$ mice had significantly decreased expression of genes for steroid biosynthesis, including estrogen biosynthesis, compared with WT mice (Table 2). Genes coding for proteins in cholesterol synthesis (*Acat2*, *Cyp2d22*, *Cyp2e1*, *Cyp2f2*, *Cyp2j9*, *Nsdhl*) and cholesterol transport (*Abca2*, *Abca5*, *Abca8a*, *Gramd1b*, *Scp2*, *Stard4*) were downregulated in *Nod2*$^{-/-}$ mice (Fig. 3 and Supplementary Table S2). The expression of genes for enzymes involved in the synthesis and activation of sex hormones (*Akr1c14*, *Akr1c18*, *Gsta3*, *Hasd17b8, Hsd17b12*, *Hsd17b14*) and signaling by these hormones (*Esr*, *Esrra*, *Ncoa1*, *Osbpl1a*, *Pgr*, *Rxra*, *Wbp2*) was also downregulated in *Nod2*$^{-/-}$ mice.

Gene expression analysis of 4T1 tumors predicted a reduction in the LXR/RXR signaling pathway in *Nod2*$^{-/-}$ mice compared with WT mice (Table 2). LXRs are nuclear receptors that bind oxysterols, and are important regulators of cholesterol, fatty acid, and glucose homeostasis. Genes that were significantly downregulated in *Nod2*$^{-/-}$ mice and regulated by LXR include many genes in lipid metabolism (*Acaca*, *Cd36*, *Echs1*, *Fasn*, *Hadh*, *Lpl*, *Osbpl1a*, *Scd1*, *Scd3*, *Srebf1*). SREBF1 is a transcription factor with a critical role in promoting the expression of genes in lipid metabolism. The lower expression of *Srebf1* in *Nod2*$^{-/-}$ mice correlates with decreased lipid metabolism in these mice. Expression of *Por*, which codes for cytochrome P450 oxidoreductase, an enzyme required for the activity of cytochrome P450 enzymes, was also significantly downregulated in *Nod2*$^{-/-}$ mice compared with WT mice (Fig. 3 and Supplementary Table S2).

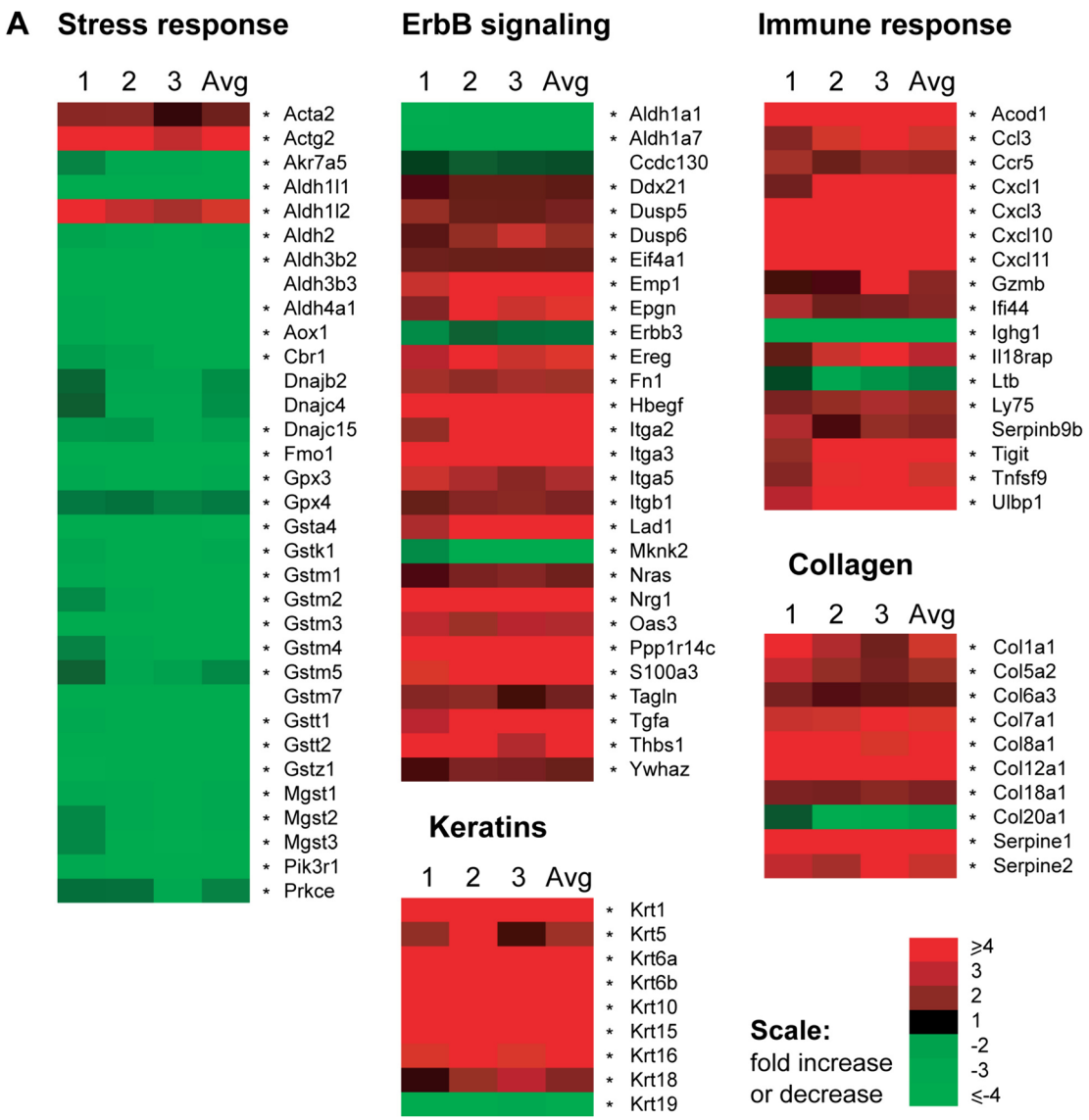
A
Stress response
1 2 3 Avg
* Acta2
* Actg2
* Akr7a5
* Aldh1l1
* Aldh1l2
* Aldh2
* Aldh3b2
Aldh3b3
* Aldh4a1
* Aox1
* Cbr1
Dnajb2
Dnajc4
* Dnajc15
* Fmo1
* Gpx3
* Gpx4
* Gsta4
* Gstk1
* Gstm1
* Gstm2
* Gstm3
* Gstm4
* Gstm5
Gstm7
* Gstt1
* Gstt2
* Gstz1
* Mgst1
* Mgst2
* Mgst3
* Pik3r1
* Prkce
ErbB signaling
1 2 3 Avg
* Aldh1a1
* Aldh1a7
Ccdc130
* Ddx21
* Dusp5
* Dusp6
* Eif4a1
* Emp1
* Epgn
* Erbb3
* Ereg
* Fn1
* Hbegf
* Itga2
* Itga3
* Itga5
* Itgb1
* Lad1
* Mknk2
* Nras
* Nrg1
* Oas3
* Ppp1r14c
* S100a3
* Tagln
* Tgfa
* Thbs1
* Ywhaz
Keratins
1 2 3 Avg
* Krt1
* Krt5
* Krt6a
* Krt6b
* Krt10
* Krt15
* Krt16
* Krt18
* Krt19
Immune response
1 2 3 Avg
* Acod1
* Ccl3
* Ccr5
* Cxcl1
* Cxcl3
* Cxcl10
* Cxcl11
* Gzmb
* Ifi44
* Ighg1
* Il18rap
* Ltb
* Ly75
Serpinb9b
* Tigit
* Tnfsf9
* Ulbp1
Collagen
1 2 3 Avg
* Col1a1
* Col5a2
* Col6a3
* Col7a1
* Col8a1
* Col12a1
* Col18a1
* Col20a1
* Serpine1
* Serpine2
Scale:
fold increase
or decrease
≥4
3
2
1
-2
-3
≤-4
B
WT
Nod2-/-
p-STAT3
p-STAT5
p-ERK1/2
Actin
C
p-STAT3
p-STAT5
p-ERK
p-STAT3 / actin
p-STAT5 / actin
p-ERK / actin
WT
Nod2-/-

◂**Fig. 5** The 4T1 tumors in *Nod2*$^{-/-}$ mice have decreased expression of genes in stress-response and increased expression of genes in ErbB signaling. **A** Heatmap representation of the fold change for gene expression in the tumors of *Nod2*$^{-/-}$ mice compared with tumors in WT mice. The genes are grouped based on pathway/function and calculated and presented as in Fig. 2. **B**, **C** Tumor homogenates were analyzed for activation of signaling molecules using antibodies to p-STAT3, p-STAT5, and p-ERK. β-Actin was used as a control. **B** Representative blot images from two experiments. **C** Band intensities were measured using ImageJ, the ratios of phosphorylated protein to actin were calculated and the mean fold changes ± SEM in *Nod2*$^{-/-}$ mice over WT are shown; $N = 10$ mice/group; significance of difference by *t-test* for *Nod2*$^{-/-}$ *versus* WT, $*P \leq 0.05$. The numerical data for individual and average RNA fold change (*Nod2*$^{-/-}$/WT) in **A** are shown in Supplementary Table S4

In addition to lipid metabolism, the expression of genes in the TCA cycle and biosynthesis of acetyl CoA were significantly inhibited in the tumors of *Nod2*$^{-/-}$ mice compared with WT mice (Table 2). *Nod2*$^{-/-}$ mice had significantly decreased expression of genes that code for enzymes in the TCA cycle (*Aco1*, *Aco2*, *Cs*, *Mdh1*, *Ogdh*, *Sdha*) and proteins in pyruvate metabolism and transport (*Pcx*, *Pdha1*, *Pdhb*, *Pdhx*, *Pdk2*, *Pdk3*, *Pdp2*, *Slc16a3*). The transport of pyruvate into the mitochondria and its conversion to acetyl CoA are critical for the TCA cycle and for the fatty acid biosynthesis. Thus, decreased transport and conversion of pyruvate would result in decreased fatty acid synthesis and the TCA cycle; and expression of genes in both pathways was lower in *Nod2*$^{-/-}$ mice compared with WT mice. Decreased expression of select genes in lipid metabolism (*Aacs*, *Acaca*, *Agpat2*, *Cpt2*, Fasn, Lipe, Plin1, Pparg, and *Scd1*) in *Nod2*$^{-/-}$ tumors compared with WT tumors was confirmed by RT-qPCR (Fig. 6B).

Thus, our results demonstrate that the 4T1 tumors in *Nod2*$^{-/-}$ mice had significantly decreased expression of genes involved in lipid and steroid metabolism and regulation compared with the tumors in WT mice.

Development of 4T1 breast tumors in *Nod2*$^{-/-}$ mice is associated with decreased expression of genes involved in adipogenesis and PPAR signaling

Gene expression analysis of 4T1 tumors also predicted a reduction of adipogenesis in the 4T1 tumors of *Nod2*$^{-/-}$ mice compared with WT mice (Table 2). *Nod2*$^{-/-}$ mice had significantly decreased expression of genes involved in the formation of lipid droplets (*Bscl2*, *Btn1a1*, *Ccdc3*, *Cidec*, *Fitm2*, *Methig1*, *Mettl7a2*, *Plin1*, *Plin4*, *Plin5)* and adipocyte metabolism (*Aacs*, *Adrb3*, *Angptl8*, *Fabp4*, *Ffar4*). Genes for proteins that promote adipocyte differentiation (*Aamdc*, *Adig*, *Angptl8*, *Apmap*, *Arxes1*, *Atf5*, *Bmp4*, *Cebpa*, Cmkir1, *Fzd4*, *Lgals12*, *Nsd2*, *Pparg*) were also downregulated in *Nod2*$^{-/-}$ mice (Fig. 4A and Supplementary Table S3).

4T1 tumors in *Nod2*$^{-/-}$ mice displayed many changes in the expression of genes involved in adipocyte signaling. Overall, these changes suggest an inhibition of adipogenesis and increased adipocyte dedifferentiation. These mice had increased expression of genes for the adipokine apelin and its receptor (*Apln*, *Aplnr*), an inhibitor of adipogenesis. In contrast, the expression of genes for the adipokine adiponectin (*Adipoq*) and its receptor (*Adipor2*), which regulate metabolism in adipocytes and promote adipogenesis, was significantly decreased in *Nod2*$^{-/-}$ mice. Insulin has a critical role in promoting adipocyte differentiation and genes that code for components of the insulin signaling pathway were downregulated (*Akt2*, *Fcor*, *Foxo1*, *Foxo4*, *Irs1*), whereas expression of *Fhl2*, an inhibitor of Foxo1, was upregulated (Fig. 4A and Supplementary Table S3).

Analysis of differentially expressed genes in other signaling pathways also predicted a decrease in preadipocyte proliferation and adipogenesis in *Nod2*$^{-/-}$ mice compared with WT mice. The expression of fibroblast growth factor 10 (*Fgf10*), which stimulates preadipocyte proliferation and adipogenesis, was downregulated in *Nod2*$^{-/-}$ mice. The expression of the Wnt receptor frizzled 6 (*Fzd6*), which is often increased in triple-negative breast cancer, was upregulated in *Nod2*$^{-/-}$ tumors. The expression of bone morphogenetic protein 4 (*Bmp4*), a member of the TGFβ family that promotes adipocyte maturation and differentiation, was decreased in *Nod2*$^{-/-}$ mice. The expression of *Gli3*, a transcription factor activated by Hedgehog signaling, which suppresses adipogenesis, was upregulated in *Nod2*$^{-/-}$ mice (Fig. 4A and Supplementary Table S3).

We identified regulatory molecules that are differentially expressed between WT and *Nod2*$^{-/-}$ mice. Based on the *P* value, the top 5 regulators included PPARα and PPARγ (Table 2), which are nuclear receptors that regulate transcription of genes involved in lipid and carbohydrate metabolism and cell proliferation and differentiation. PPARγ is expressed predominantly in the adipose tissue and induces expression of many genes involved in adipogenesis, including *Acox1*, *Acsl1*, *Ascl4*, *Cebpa*, *Cd36*, *Cpt2*, *Fabp4*, *Lpl*, *Plin1*, *Scd1*, *Scd4*, *Slc27a1*, *Slc27a4*, which were differentially regulated between WT and *Nod2*$^{-/-}$ mice. The transcription factor CEBPα also plays a critical role in promoting adipocyte growth and differentiation. The expression of *Cebpa* and its activator *Atf5* were both significantly decreased in *Nod2*$^{-/-}$ mice. The expression of *Foxc2*, a transcription factor associated with epithelial to mesenchymal transition, was upregulated in *Nod2*$^{-/-}$ mice (Fig. 4 and Supplementary Table S3). Our STRING analysis further demonstrates that many of the differentially regulated genes in adipogenesis are regulated by PPARγ (Fig. 4B). Furthermore, 4T1 tumors in *Nod2*$^{-/-}$ mice had significantly lower levels of total triglyceride and cholesterol compared with WT mice (Fig. 4C).

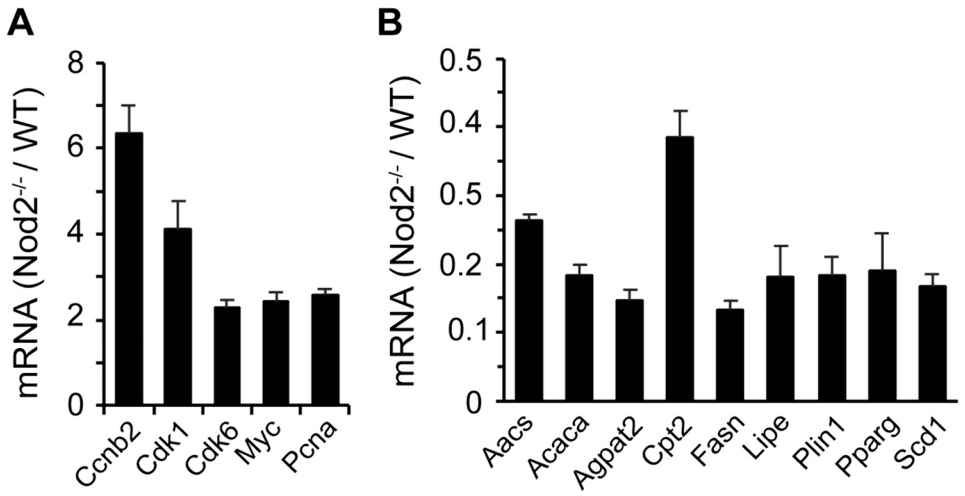

Fig. 6 The 4T1 tumors in *Nod2*$^{-/-}$ mice have **A** increased expression of genes involved in cell cycle and **B** decreased expression of genes in lipid metabolism. Changes in the expression of select genes was confirmed by RT-qPCR and the ratio of mRNA (fold change) in *Nod2*$^{-/-}$ tumors to WT tumors is shown. The results are means ± SEM from 5 mice per group and all changes are significant by t-Test ($p < 0.05$). The primers used for qPCR are shown in Table S5

Our results demonstrate that the development of 4T1 tumors in *Nod2*$^{-/-}$ mice was associated with a dramatic decrease in the expression of genes involved in lipid metabolism and adipogenesis, which was accompanied by reduced lipid content.

Development of 4T1 breast tumors in *Nod2*$^{-/-}$ mice is associated with decreased expression of stress-response genes and increased ErbB signaling

Gene expression analysis of 4T1 tumors also predicted a reduction of glutathione-mediated detoxification and Nrf2-mediated oxidative stress response pathways in *Nod2*$^{-/-}$ mice compared with WT mice (Table 2). Nrf2 is a transcription factor that induces the expression of genes involved in detoxification reactions. *Nod2*$^{-/-}$ mice had significantly decreased expression of genes for glutathione peroxidase (*Gpx3*, *Gpx4*), members of the glutathione S-transferase family (*Gsta3*, *Gsta4*, *Gstk1*, *Gstm1, Gstm2, Gstm3, Gstm4, Gstm5*), microsomal glutathione S-transferase (*Mgst1*, *Mgst2*, *Mgst3*), members of the aldehyde dehydrogenase family (*Aldh1l1*, *Aldh1l2*, *Aldh2*, *Aldh3b2*, *Aldh3b3*, *Aldh4a1*), and heat shock proteins (*Dnajb2*, *Dnajc4*, *Dnajc15*) (Fig. 5A and Supplementary Table S4).

Transcriptomic data predicted increased activation of the ErbB signaling pathway in *Nod2*$^{-/-}$ tumors compared with WT tumors (Table 2). The ErbB receptor tyrosine kinase family consists of four cell surface receptors, ErbB1, ErbB2, ErbB3, and ErbB4, and plays a critical role in many cancers. There was no significant difference in the expression of *ErbB1*, *ErbB2*, and *ErbB4* between *Nod2*$^{-/-}$ and WT mice, whereas the expression of *ErbB3* was significantly decreased in *Nod2*$^{-/-}$ mice (Fig. 5 and Supplementary Table S4). However, *Nod2*$^{-/-}$ mice had significantly increased gene expression of ligands that bind and activate ErbB receptors (*Epgn*, *Ereg*, *Hbegf*, *Nrg1*, *Tgfa*) and downstream targets, including phosphatases that inhibit the MAP kinase pathway (*Dusp5*, *Dusp6*) and integrin subunits (*Itga2*, *Itga3*, *Itga5*, *Itgb1*) (Fig. 5A and Supplementary Table S4).

The role of *Nod2* in innate immunity and inflammation is well characterized. A deficiency in *Nod2* is linked to increased inflammation and the development of Crohn's disease and colorectal cancer and may also contribute to the development of obesity and hepatocellular carcinoma [7, 8, 20–23]. However, in our breast cancer model, *Nod2*$^{-/-}$ mice did not develop a strong immune response. There were only a few immune response genes differentially expressed between WT and *Nod2*$^{-/-}$ mice. *Nod2*$^{-/-}$ mice had significantly higher expression of the chemokine genes, *Ccl3*, *Cxcl1*, *Cxcl3*, *Cxcl10* and *Cxcl11*, which suggests that there may be increased neutrophil and macrophage infiltration in the tumors of these mice. *Nod2*$^{-/-}$ mice also had higher expression of aconitate decarboxylase (*Acod1*) gene (Fig. 5A and Supplementary Table S4), which converts cis-aconitate to itaconate, a metabolite that mediates crosstalk between innate immunity and metabolism and is elevated in certain tumors [33].

We further identified differences in the expression of keratins and collagens between WT and *Nod2*$^{-/-}$ mice. Keratins (cytokeratins) are the major cytoskeletal proteins in epithelial cells and include ~ 20 different proteins, whereas collagens are the predominant proteins in the extracellular matrix and include ~ 28 different proteins. The expression of individual keratins and collagens is frequently altered in cancer and specific changes help differentiate between subtypes of a cancer [34]. The 4T1 tumors in *Nod2*$^{-/-}$ mice had significantly higher expression of genes for several keratins, including *Krt1*, *Krt6a*, *Krt6b*, *Krt10*, *Krt15*, *Krt16*, several collagens, including *Col1a1*, *Col6a3*, *Col8a1*, and *Col12a1*, and inhibitors of proteases (*Serpine1*, *Serpine2*)

that modify the extracellular matrix (Fig. 5A and Supplementary Table S4).

We next analyzed the activation of STAT3, STAT5, and ERK1/2, which are activated by multiple signaling pathways, including ErbB, and are often activated in many cancers. *Nod2*$^{-/-}$ mice had significantly higher levels of p-STAT3, lower levels of p-STAT5 and no difference in levels of p-ERK1/2 compared with WT mice (Fig. 5B and C). These results correlate with the decreased expression of *Stat5a* (Fig. 3) and the increased expression of MAPK inhibitors (*Dusp5*, *Dusp6*) in *Nod2*$^{-/-}$ mice (Fig. 5A).

Development of 4T1 breast tumors in *Nod2*$^{-/-}$ mice is associated with altered expression of genes associated with cancer

We next determined whether the genes differentially activated in *Nod2*$^{-/-}$ mice (Table 1 and Figs. 2, 3, 4, and 5) have been previously identified in cancer patients or in cancer models. We searched for these genes in different databases including PubMed and GeneCards. The vast majority of the differentially expressed genes between WT and *Nod2*$^{-/-}$ mice have been previously identified either in cancer patients, including breast cancer, or in cancer models (Table 3). These genes are marked with an asterisk in the heat maps (Figs. 2, 3, 4, and 5).

Discussion

Breast cancer patients exhibit great variation in the development and progression of tumors and in their response to treatment. This diversity is largely determined by differences in the transcriptional profile of tumors among patients and current management strategies are often based upon obtaining a molecular signature of the tumor [3, 4]. Despite this approach, the treatment success rate is low, as genetic contributions to the development and treatment of breast cancer are not completely understood. Thus, a comprehensive understanding of the differences in gene expression among different breast cancer subtypes is essential for developing more effective treatments.

Chronic inflammation plays an important role in all stages of tumor development, including initiation, growth, invasion, and metastasis [35–37]. There is dynamic crosstalk between cancer and innate immune cells, which may induce antitumor immunity or promote tumor development. *Nod2* is a key player in innate immune responses to bacteria, and emerging evidence shows that *Nod2* is also involved in the susceptibility to and development of colorectal cancer and hepatocellular carcinoma [15–17, 23, 24]. Further, the *Nod2* variant 3020insC is significantly associated with early onset of breast cancer [25, 38]. However, the role of *Nod2* in the development of breast cancer has not been demonstrated.

In the current study, we tested the hypothesis that *Nod2*-deficient mice are more susceptible to the development of breast tumors. We used an orthotopic model for this study and demonstrated that *Nod2*$^{-/-}$ mice injected with 4T1 mammary carcinoma cells developed significantly larger tumors than similarly treated WT mice. The incidence of disease was also significantly higher in *Nod2*$^{-/-}$ mice; 100% of 4T1 *Nod2*$^{-/-}$ mice, but only 50% of WT mice, developed tumors.

We performed a comprehensive analysis of changes in gene expression in the tumors of WT and *Nod2*$^{-/-}$ mice to identify pathways that are predicted to be differentially activated. Within these pathways, we next identified genes that were differentially expressed and showed that the tumors in *Nod2*$^{-/-}$ mice have significantly increased expression of genes involved in DNA replication and repair pathways compared with WT mice. There were 80 genes included in this panel and 98% of these genes had increased expression in *Nod2*$^{-/-}$ mice compared with WT mice. Most of these genes

Table 3 Genes differentially expressed in 4T1 tumors of *Nod2*$^{-/-}$ mice compared with WT mice that were previously shown to be associated with cancer

Pathways	Number of genes with ≥ twofold change (Nod2$^{-/-}$/WT), P ≤ 0.05	% Genes associated with cancer
DNA replication and repair	80	100
Cell cycle	105	97
Lipolysis	53	91
Lipogenesis	55	84
Steroid biosynthesis & signaling	45	91
Pyruvate metabolism & TCA cycle	18	100
Adipogenesis	49	73
ErbB signaling	28	96
Stress response	34	88
Immune response	17	94
Keratins	9	100
Collagen and protease inhibitors	10	100

are required for and/or promote DNA replication and repair. *Nod2*$^{-/-}$ mice also showed significantly increased expression of genes for cell cycle and cell proliferation pathways; 93% of the 105 genes in this panel had increased expression in *Nod2*$^{-/-}$ mice. Most of these upregulated genes are required for and/or promote cell cycle and genes that were downregulated are inhibitors of the cell cycle. Thus, the overwhelming effect of the changes in gene expression in *Nod2*$^{-/-}$ mice likely promotes DNA replication and cell division, which is consistent with the development of larger tumors and higher incidence of tumors in *Nod2*$^{-/-}$ mice.

Metabolic reprogramming is one of the hallmarks of cancer, as rapidly proliferating cells have increased energy and macromolecule requirements [35, 39]. Both cancer and surrounding cells undergo profound changes in metabolism during tumorigenesis and these changes affect the proliferation, invasion, and metastasis of the tumor. The tumors in *Nod2*$^{-/-}$ mice had decreased lipogenesis and lipolysis compared with WT mice. *Nod2*$^{-/-}$ mice exhibited an overwhelmingly decreased level of expression of genes for proteins required for the biosynthesis of fatty acids, triglycerides and glycerophospholipids; 93% of the 55 genes in the lipogenesis panel had decreased expression. Additionally, there was a decreased expression of genes for proteins required for fatty acid oxidation (both mitochondrial and peroxisomal) and breakdown of triglycerides. 96% of the 53 genes included in the lipolysis panel had a decreased expression in *Nod2*$^{-/-}$ mice. Expression of genes involved in steroid biosynthesis and steroid signaling were also downregulated in *Nod2*$^{-/-}$ mice; 91% of the 45 genes included in this panel had a decreased expression compared with WT mice.

The changes in lipid metabolism were accompanied by a strong decrease in the expression of genes involved in adipogenesis in *Nod2*$^{-/-}$ mice compared with WT mice. *Nod2*$^{-/-}$ mice had decreased expression of genes required for the formation of lipid droplets and for markers of mature adipocytes. Insulin signaling and activation of downstream proteins, such as Foxo1, are essential for adipocyte differentiation [40]. There was a reduced expression of genes in the insulin signaling pathway and its downstream targets. The expression of genes for the key transcription factors that promote adipogenesis, PPARγ and C/EBPα, was also decreased in *Nod2*$^{-/-}$ mice. These changes in gene expression were accompanied with decreased levels of both triglycerides and cholesterol in the tumors of *Nod2*$^{-/-}$ mice.

The 4T1 cells were injected into the fat pad of the mammary gland and adipocytes likely are part of the tumor microenvironment. Solid tumors are often found near white adipose tissue (WAT), which is a key player in tumor progression. On exposure to cancer cells, adipocytes undergo delipidation and dedifferentiation and acquire a fibroblast-like morphology. Delipidation provides the fuel necessary for the proliferation of cancer cells and increased dedifferentiation of adipocytes is associated with aggressive tumors [40–42]. Thus, our results suggest that in *Nod2*$^{-/-}$ mice, adipocytes in the tumor microenvironment rapidly undergo dedifferentiation and delipidation. These changes likely support the rapid growth of 4T1 tumors in *Nod2*$^{-/-}$ mice.

This process of dedifferentiation and delipidation of WAT is often accompanied by increased inflammatory markers, TNFα, IL6, IL1α, and IL1β. However, there was no difference in the gene expression for these proteins between WT and *Nod2*$^{-/-}$ mice. Despite the role of *Nod2* in modulating immune responses and inflammation, there was only a mild increase in the expression of genes involved in the immune response in the tumors of *Nod2*$^{-/-}$ mice compared with WT mice. Thus, inflammation may not play a significant role in the higher incidence and larger size of tumors in *Nod2*$^{-/-}$ mice.

Murine 4T1 tumors are similar to triple-negative breast cancer (TNBC) in humans, as they express low levels of estrogen, progesterone, and ErbB2 receptors. Similarly, the gene expression of these three receptors was also low in *Nod2*$^{-/-}$ tumors. There are different subtypes of TNBC tumors: BL1 and BL2, which are heavily enriched in cell cycle and DNA replication pathways and growth factor signaling; IM subtype, which is enriched in immune cell processes and cytokine and chemokine signaling; M and MSL subtypes, which are enriched in cell motility and cellular differentiation; and LAR subtype, which is enriched in hormonally regulated pathways, including steroid biosynthesis, porphyrin metabolism and androgen/estrogen metabolism [34]. There is also differential expression of keratins within these subtypes [34]. 4T1 tumors in *Nod2*$^{-/-}$ mice resemble the BL1 and BL2 TNBC subtypes with a gene expression signature that is enriched for cell cycle and DNA replication, reduced for steroid biosynthesis, steroid signaling, and immune response, and increased expression of *Krt5*, *Krt6a*, *Krt6b*, and *Krt16* genes.

We further demonstrate that *Nod2*$^{-/-}$ mice had increased levels of activated STAT3, a transcription factor that is frequently activated in breast cancer [43]. By contrast, activation, and expression of STAT5 were decreased in *Nod2*$^{-/-}$ mice and inhibition of this transcription factor have been observed in breast cancer patients [43, 44].

The importance of *Nod2* in bacterial innate immune responses, inflammation, and colitis is well established [7, 8]. There is also increasing evidence that *Nod2* regulates metabolism, as *Nod2*$^{-/-}$ mice are more prone to the development of diet-dependent obesity, hepatic and adipose tissue inflammation, and liver cancer [12, 20–24]. However, the mechanisms by which *Nod2* modulates the development of these diseases are not well understood. One proposed explanation for the increased inflammation associated with *Nod2* deficiency is that Nod2 suppresses signaling through

TLRs, which are major contributors to inflammation. In the absence of *Nod2*, TLR activation is unchecked, which results in hyperinflammation [19, 45–47]. A second parallel mechanism that may contribute to the development of diet-dependent obesity and hepatic malignancy in *Nod2*$^{-/-}$ mice may be the recently described Nod2-mediated activation of AMPK [24]. In this study, the authors show that *Nod2* protects from *N*-nitrosodiethylamine/carbon tetrachloride-induced hepatocarcinogenesis and that in hepatic tumor cell lines, Nod2 binds to and activates AMPK signaling, which inhibits mTORC1 resulting in an anti-tumor effect [24]. However, these in vitro results have not been confirmed in vivo. AMPK is a master regulator of metabolism and cell proliferation, and changes in the activation of AMPK contribute to many diseases, including breast cancer [48, 49].

The development of breast cancer in *Nod2*$^{-/-}$ mice is associated with an overwhelming increase in the expression of genes associated with DNA replication and cell cycle, an overwhelming decrease in the expression of genes associated with lipid metabolism, and a few changes in the expression of genes associated with immune response. These changes may be fueled by increased dedifferentiation and delipidation of surrounding adipocytes. Based on these changes, we hypothesize that the role of *Nod2* in regulating AMPK may contribute to the development of breast cancer. Our future studies will focus on the verification of this hypothesis.

Conclusion

We have demonstrated that the pattern recognition receptor *Nod2* protects mice from tumors in an orthotopic model of mammary carcinoma. Our results indicate that *Nod2* is essential for maintaining optimal levels of DNA replication, cell growth and division, lipid metabolism, and adipogenesis. A *Nod2* deficiency combined with stress (transplanted carcinoma cells) results in increased expression of genes that likely promote DNA replication and cell division and decreased expression of genes required for lipid metabolism and adipogenesis. These imbalances likely lead to increased sensitivity to and rapid development of orthotopic tumors in *Nod2*$^{-/-}$ mice. Our results further support growing evidence that *Nod2* possesses other functions, besides immune responses to bacterial peptidoglycan, and that *Nod2* is required for maintaining cellular homeostasis in response to different stresses. Thus, we demonstrate that the genetic background (the presence or absence of functional *Nod2*) affects the host's sensitivity to breast cancer and, therefore, the *Nod2*$^{-/-}$ orthotopic tumor model may provide a novel in vivo system for the study of molecular changes associated with various subtypes of breast cancer, and for testing the effectiveness of therapeutic drugs in genetically different hosts.

Supplementary Information The online version contains supplementary material available at https://doi.org/10.1007/s11033-024-09927-2.

Acknowledgements We are grateful to Julie Cook for maintaining and breeding our mice.

Author contributions Conceptualization, DG; methodology, SG, NV, DG; software, SG, DG; formal analysis, SG, NV, DG; investigation, SG, NV, DG; resources, DG; data curation, SG, DG; writing original draft, DG; writing—reviewing and editing, SG, NV, DG; visualization, SG, NV, DG; supervision, DG; project administration, DG; funding acquisition, DG. All authors have read and agreed to the published version of the manuscript.

Funding No external funds were received for this project.

Data availability All supporting transcriptomic data have been deposited in NCBI's Gene Expression Omnibus, Accession number GSE207617.

Declarations

Conflict of interest The authors have no relevant financial or non-financial interests to disclose.

Ethical approval All animal experiments in this study were approved by the Institutional Review Board of Indiana University School of Medicine-Northwest (protocol code NW-45).

References

1. Houghton SC, Hankinson SE (2021) Cancer progress and priorities: breast cancer. Cancer Epidemiol Biomarkers Prev 30(5):822–844
2. Siegel RL, Miller KD, Jemal A (2019) Cancer statistics, 2019. CA Cancer J Clin 69(1):7–34
3. Perou CM, Sorlie T, Eisen MB, van de Rijn M, Jeffrey SS, Rees CA, Pollack JR, Ross DT, Johnsen H, Akslen LA et al (2000) Molecular portraits of human breast tumours. Nature 406(6797):747–752
4. Solanki M, Visscher D (2020) Pathology of breast cancer in the last half century. Hum Pathol 95:137–148
5. Michailidou K, Lindstrom S, Dennis J, Beesley J, Hui S, Kar S, Lemacon A, Soucy P, Glubb D, Rostamianfar A et al (2017) Association analysis identifies 65 new breast cancer risk loci. Nature 551(7678):92–94

6. Litton JK, Burstein HJ, Turner NC (2019) Molecular testing in breast cancer. Am Soc Clin Oncol Educ Book 39:e1–e7
7. Caruso R, Warner N, Inohara N, Nunez G (2014) NOD1 and NOD2: signaling, host defense, and inflammatory disease. Immunity 41(6):898–908
8. Philpott DJ, Sorbara MT, Robertson SJ, Croitoru K, Girardin SE (2014) NOD proteins: regulators of inflammation in health and disease. Nat Rev Immunol 14(1):9–23
9. Girardin SE, Boneca IG, Viala J, Chamaillard M, Labigne A, Thomas G, Philpott DJ, Sansonetti PJ (2003) Nod2 is a general sensor of peptidoglycan through muramyl dipeptide (MDP) detection. J Biol Chem 278(11):8869–8872
10. Inohara N, Ogura Y, Fontalba A, Gutierrez O, Pons F, Crespo J, Fukase K, Inamura S, Kusumoto S, Hashimoto M et al (2003) Host recognition of bacterial muramyl dipeptide mediated through NOD2. Implications for Crohn's disease. J Biol Chem 278(8):5509–5512
11. Keestra-Gounder AM, Tsolis RM (2017) NOD1 and NOD2: beyond peptidoglycan sensing. Trends Immunol 38:758–767
12. Zangara MT, Johnston I, Johnson EE, McDonald C (2021) Mediators of metabolism: an unconventional role for NOD1 and NOD2. Int J Mol Sci 22(3):1156
13. Hugot JP, Chamaillard M, Zouali H, Lesage S, Cezard JP, Belaiche J, Almer S, Tysk C, O'Morain CA, Gassull M et al (2001) Association of NOD2 leucine-rich repeat variants with susceptibility to Crohn's disease. Nature 411(6837):599–603
14. Ogura Y, Bonen DK, Inohara N, Nicolae DL, Chen FF, Ramos R, Britton H, Moran T, Karaliuskas R, Duerr RH et al (2001) A frameshift mutation in NOD2 associated with susceptibility to Crohn's disease. Nature 411(6837):603–606
15. Kurzawski G, Suchy J, Kladny J, Grabowska E, Mierzejewski M, Jakubowska A, Debniak T, Cybulski C, Kowalska E, Szych Z et al (2004) The NOD2 3020insC mutation and the risk of colorectal cancer. Cancer Res 64(5):1604–1606
16. Tian Y, Li Y, Hu Z, Wang D, Sun X, Ren C (2010) Differential effects of NOD2 polymorphisms on colorectal cancer risk: a meta-analysis. Int J Colorectal Dis 25(2):161–168
17. Branquinho D, Freire P, Sofia C (2016) NOD2 mutations and colorectal cancer—where do we stand? World J Gastrointest Surg 8(4):284–293
18. Couturier-Maillard A, Secher T, Rehman A, Normand S, De Arcangelis A, Haesler R, Huot L, Grandjean T, Bressenot A, Delanoye-Crespin A et al (2013) NOD2-mediated dysbiosis predisposes mice to transmissible colitis and colorectal cancer. J Clin Invest 123(2):700–711
19. Udden SMN, Peng L, Gan JL, Shelton JM, Malter JS, Hooper LV, Zaki MH (2017) NOD2 suppresses colorectal tumorigenesis via downregulation of the TLR pathways. Cell Rep 19(13):2756–2770
20. Rodriguez-Nunez I, Caluag T, Kirby K, Rudick CN, Dziarski R, Gupta D (2017) Nod2 and Nod2-regulated microbiota protect BALB/c mice from diet-induced obesity and metabolic dysfunction. Sci Rep 7(1):548
21. Denou E, Lolmede K, Garidou L, Pomie C, Chabo C, Lau TC, Fullerton MD, Nigro G, Zakaroff-Girard A, Luche E et al (2015) Defective NOD2 peptidoglycan sensing promotes diet-induced inflammation, dysbiosis, and insulin resistance. EMBO Mol Med 7(3):259–274
22. Cavallari JF, Fullerton MD, Duggan BM, Foley KP, Denou E, Smith BK, Desjardins EM, Henriksbo BD, Kim KJ, Tuinema BR et al (2017) Muramyl dipeptide-based postbiotics mitigate obesity-induced insulin resistance via IRF4. Cell Metab 25(5):1063-1074 e1063
23. Gurses SA, Banskar S, Stewart C, Trimoski B, Dziarski R, Gupta D (2020) Nod2 protects mice from inflammation and obesity-dependent liver cancer. Sci Rep 10(1):20519
24. Ma X, Qiu Y, Sun Y, Zhu L, Zhao Y, Li T, Lin Y, Ma D, Qin Z, Sun C et al (2020) NOD2 inhibits tumorigenesis and increases chemosensitivity of hepatocellular carcinoma by targeting AMPK pathway. Cell Death Dis 11(3):174
25. Huzarski T, Lener M, Domagala W, Gronwald J, Byrski T, Kurzawski G, Suchy J, Chosia M, Woyton J, Ucinski M et al (2005) The 3020insC allele of NOD2 predisposes to early-onset breast cancer. Breast Cancer Res Treat 89(1):91–93
26. Velloso FJ, Sogayar MC, Correa RG (2018) Expression and in vitro assessment of tumorigenicity for NOD1 and NOD2 receptors in breast cancer cell lines. BMC Res Notes 11(1):222
27. Velloso FJ, Campos AR, Sogayar MC, Correa RG (2019) Proteome profiling of triple negative breast cancer cells overexpressing NOD1 and NOD2 receptors unveils molecular signatures of malignant cell proliferation. BMC Genom 20(1):152
28. Kocaturk B, Versteeg HH (2015) Orthotopic injection of breast cancer cells into the mammary fat pad of mice to study tumor growth. J Vis Exp 96:51967
29. Paschall AV, Liu K (2016) An orthotopic mouse model of spontaneous breast cancer metastasis. J Vis Exp 14:54040
30. Nanni P, de Giovanni C, Lollini PL, Nicoletti G, Prodi G (1983) TS/A: a new metastasizing cell line from a BALB/c spontaneous mammary adenocarcinoma. Clin Exp Metastasis 1(4):373–380
31. Love MI, Huber W, Anders S (2014) Moderated estimation of fold change and dispersion for RNA-seq data with DESeq2. Genome Biol 15(12):550
32. Szklarczyk D, Gable AL, Lyon D, Junge A, Wyder S, Huerta-Cepas J, Simonovic M, Doncheva NT, Morris JH, Bork P et al (2019) STRING v11: protein-protein association networks with increased coverage, supporting functional discovery in genome-wide experimental datasets. Nucleic Acids Res 47(D1):D607
33. Weiss JM, Davies LC, Karwan M, Ileva L, Ozaki MK, Cheng RY, Ridnour LA, Annunziata CM, Wink DA, McVicar DW (2018) Itaconic acid mediates crosstalk between macrophage metabolism and peritoneal tumors. J Clin Invest 128(9):3794–3805
34. Lehmann BD, Bauer JA, Chen X, Sanders ME, Chakravarthy AB, Shyr Y, Pietenpol JA (2011) Identification of human triple-negative breast cancer subtypes and preclinical models for selection of targeted therapies. J Clin Invest 121(7):2750–2767
35. Hanahan D, Weinberg RA (2011) Hallmarks of cancer: the next generation. Cell 144(5):646–674
36. Gajewski TF, Schreiber H, Fu YX (2013) Innate and adaptive immune cells in the tumor microenvironment. Nat Immunol 14(10):1014–1022
37. Hagerling C, Casbon AJ, Werb Z (2015) Balancing the innate immune system in tumor development. Trends Cell Biol 25(4):214–220
38. Huszno J, Kolosza Z, Nycz-Bochenek M, Lisik M, Mazur M, Pamula-Pilat J, Grzybowska E (2020) Clinicopathological characteristics of breast cancer patients with NOD2 mutation according to age. Contemp Oncol (Pozn) 24(2):79–86
39. Penkert J, Ripperger T, Schieck M, Schlegelberger B, Steinemann D, Illig T (2016) On metabolic reprogramming and tumor biology: a comprehensive survey of metabolism in breast cancer. Oncotarget 7(41):67626–67649
40. Rybinska I, Mangano N, Tagliabue E, Triulzi T (2021) Cancer-associated adipocytes in breast cancer: causes and consequences. Int J Mol Sci 22(7):3775
41. Zhao C, Wu M, Zeng N, Xiong M, Hu W, Lv W, Yi Y, Zhang Q, Wu Y (2020) Cancer-associated adipocytes: emerging supporters in breast cancer. J Exp Clin Cancer Res 39(1):156
42. Triulzi T (2021) Special issue: "unraveling the involvement of adipose tissue in breast cancer progression." Int J Mol Sci 22(10):5107

43. Furth PA (2014) STAT signaling in different breast cancer subtypes. Mol Cell Endocrinol 382(1):612–615
44. Mukhopadhyay UK, Cass J, Raptis L, Craig AW, Bourdeau V, Varma S, Gupta SS, Elliott BE, Ferbeyre G (2016) Dataset of STAT5A status in breast cancer. Data Brief 7:490–492
45. Watanabe T, Kitani A, Murray PJ, Strober W (2004) NOD2 is a negative regulator of toll-like receptor 2-mediated T helper type 1 responses. Nat Immunol 5(8):800–808
46. Watanabe T, Kitani A, Strober W (2005) NOD2 regulation of toll-like receptor responses and the pathogenesis of Crohn's disease. Gut 54(11):1515–1518
47. Watanabe T, Kitani A, Murray PJ, Wakatsuki Y, Fuss IJ, Strober W (2006) Nucleotide binding oligomerization domain 2 deficiency leads to dysregulated TLR2 signaling and induction of antigen-specific colitis. Immunity 25(3):473–485
48. Mihaylova MM, Shaw RJ (2011) The AMPK signalling pathway coordinates cell growth, autophagy and metabolism. Nat Cell Biol 13(9):1016–1023
49. Zhao H, Orhan YC, Zha X, Esencan E, Chatterton RT, Bulun SE (2017) AMP-activated protein kinase and energy balance in breast cancer. Am J Transl Res 9(2):197–213